

On ultrafast magnetic flux dendrite propagation into thin superconducting films

B. Biehler, B.-U. Runge, and P. Leiderer

Physics Department, University of Konstanz, D-78457 Konstanz, Germany

R. G. Mints*

*School of Physics and Astronomy, Raymond and Beverly Sackler
Faculty of Exact Sciences, Tel Aviv University, Tel Aviv 69978, Israel*

(Dated: November 20, 2018)

We suggest a new theoretical approach describing the velocity of magnetic flux dendrite penetration into thin superconducting films. The key assumptions for this approach are based upon experimental observations. We treat a dendrite tip motion as a propagating flux jump instability. Two different regimes of dendrite propagation are found: A fast initial stage is followed by a slow stage, which sets in as soon as a dendrite enters into the vortex-free region. We find that the dendrite velocity is inversely proportional to the sample thickness. The theoretical results and experimental data obtained by a magneto-optic pump-probe technique are compared and excellent agreement between the calculations and measurements is found.

PACS numbers: 74.25.Fy, 74.40.+k, 74.78.Bz

Keywords: flux dendrite, flux jumps, flux penetration

Magnetic flux penetration in type-II superconductors is successfully described by the Bean critical state model [1]. This model assumes that the slope of the flux “hills” is given by $\mu_0 j_c(T, B)$, where the critical current density $j_c(T, B)$ is a decreasing function of the temperature T and field B . Bean’s critical state with its spatially nonuniform flux distribution is not at equilibrium and under certain conditions the smooth flux penetration process becomes unstable (see review [2] and references therein). The spatial and temporal development of this instability depends on the sample geometry, temperature, external magnetic field, its rate of change and orientation, initial and boundary conditions, etc.

Instabilities in the critical state result in flux redistribution towards the equilibrium state (spatially homogeneous flux throughout the sample) and are accompanied by a significant heat release, which often leads to the superconductor-to-normal-transition. The basic instability observed in Bean’s critical state is the flux jump instability, which was discovered already in the early experiments on superconductors with strong pinning [2].

The basic physics of flux jumping can be easily illustrated. Assume a perturbation of temperature or flux occurring in Bean’s critical state. This perturbation can be caused by an external reason or a spontaneous fluctuation arising in the system itself. The initial perturbation redistributes the magnetic flux inside the superconductor. This flux motion by itself induces an electric field which leads to dissipation, since the electric field does not only act on the Cooper pairs but also on the unpaired electrons. This additional dissipation results in an extra heating which in turn leads to an additional flux motion. This “loop” establishes a positive feedback driving the system towards the equilibrium state. The flux jumping instability exhibits itself as suddenly appearing flux avalanche (flux jump) and heat release [2, 3].

Spatially resolved flux front patterns of Bean’s critical state instability were first observed in Nb discs with thicknesses in the range of $d \approx 10^{-5}$ m to 10^{-3} m by means of magneto-optic imaging [4]. Wertheimer and Gilchrist discovered a well defined pattern of flux dendrites with a width $w \sim 10^{-3}$ m and propagation velocity v in the interval between 5 m/s and 100 m/s [4]. The dendrites velocity depended on the disks thickness, for smaller d a higher v was found.

The modern magneto-optic technique allowing to investigate flux patterns with time resolution on the order of ≈ 100 ps [5, 6] stimulated quite a few experimental and theoretical studies of flux front patterns arising in a process of smooth flux penetration [7] as well as in a process of critical state instability development in superconducting films in a transversal magnetic field. Different scenarios are considered resulting in a variety of flux patterns, e.g., magnetic turbulence [8, 9], kinetic flux front roughening [10], magnetic micro avalanches [11, 12], flux dendrites [13, 14, 15, 16, 17], thermomagnetic fingering [18], bending of flux-antiflux interface [19, 20], and flux front corrugation [21].

A wealth of recent experiments convincingly demonstrate that a propagating dendritic flux pattern driven by the flux jumping instability is a general phenomenon typical for Bean’s-type critical state [13, 14, 15, 22, 23, 24, 25]. Indeed, the flux dendrites were observed under a wide variety of conditions in superconducting films of Nb [13, 14, 22], $\text{YBa}_2\text{Cu}_3\text{O}_{7-\delta}$ [13, 15, 23], Nb_3Sn [24], and MgB_2 [25].

It is known, that dendrite propagation in thin films shows velocities up to 160 km/s [15], *i.e.*, these velocities are much higher than the speed of sound. This ultrafast motion of flux dendrites in thin superconducting films is a long standing and challenging problem.

In this letter we derive a novel equation for a dendrite

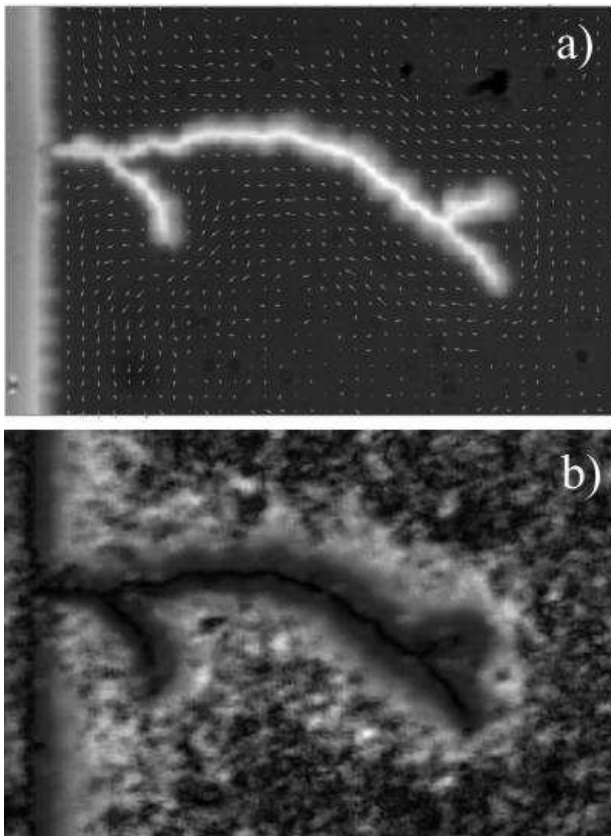


FIG. 1: Magneto-optic images of a dendritic flux pattern in a YBCO film with the thickness $d = 330$ nm subjected to a field of $B_a = 15$ mT. (a) Final state (after ≈ 10 s) of a dendritic flux pattern with superimposed current distribution shown by the arrows. The length of the arrows is proportional to the local current density. (b) The absolute value of the current density is shown. The bright areas indicate high current densities.

tip velocity and demonstrate an excellent agreement between the theoretical results and experimental data for the propagation velocity of a single flux dendrite branch.

Dendritic flux structures which can be considered as a set of single flux branches originating from a certain area were observed in numerous experiments [15]. In the case of a dendritic structure with few branches the single branches do not affect each other and the propagating substructures can be treated as a moving flux jump instability localized at the tip of the dendrite branches. A typical magneto-optic image of a “dilute” dendrite in its final state is shown in Fig. 1(a). Superimposed are the current streamlines as determined by an inversion scheme [30]. In Fig. 1(b) the absolute value of the current density is shown. It is worth mentioning that the center of the dendrite is current free and that the current follows the dendrite branches. The current density decreases rapidly with distance from the dendritic structure.

These experimental observations allow for a straight-line flux dendrite model, which we use in our calculations.

This model assumes the following:

(a) The current of a straight-line dendrite first flows parallel to the sample edge, then closely follows the contour of the dendrite branch until flowing parallel to the sample edge again as shown in Fig. 2.

(b) In the current carrying areas, the superconductor is in the flux creep regime and thus the current density j depends on the electric field E as

$$j = j_c (E/E_0)^{1/n}, \quad (1)$$

where j_c is the critical current density, n and E_0 are the parameters characterizing the current density-electric field curve (at $E = E_0$ we have $j = j_c$). It is common to define j_c as the current density at $E_0 = 10^{-4}$ V/m, for high- T_c superconductors $n \sim 10$ but decreases with the applied magnetic field [29]. Eq. (1) yields the electric field dependent conductivity

$$\sigma(E) = \frac{dj}{dE} \approx \frac{j_c}{nE}. \quad (2)$$

Next, we denote the radius of the dendrite tip as ρ_0 and the width of the current carrying area as

$$\rho_p = B_{\text{eff}}/\mu_0 j_c, \quad (3)$$

where $B_{\text{eff}} = B_{\text{in}} - B_{\text{out}}$, B_{in} is the field inside the dendrite, and B_{out} is the field outside the tip of the dendrite.

Consider now the flux front stability at a tip of a moving flux dendrite in the framework of the model developed to treat the flux jump instability near a semicircle indentation at the sample edge [26, 27, 28]. This approach is based on the assumption that the flux jumping instability develops much faster than the magnetic flux diffusion. In the flux creep regime of low- T_c and high- T_c superconductors this assumption holds with a high accuracy [26, 27].

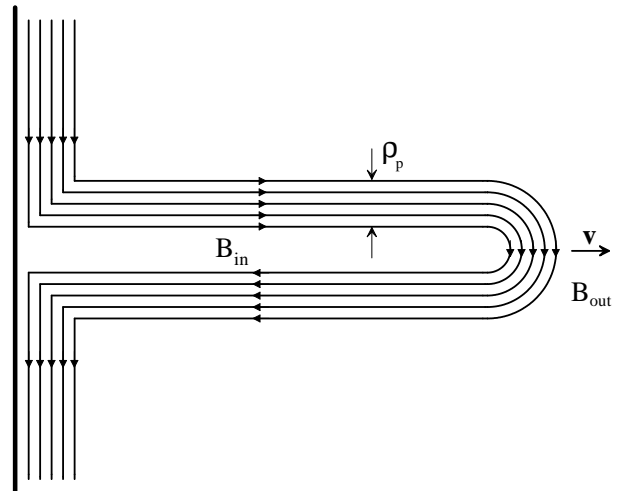


FIG. 2: Current lines for the straight-line magnetic flux dendrite. The full line to the left marks the strip edge.

It follows from the general approach that the stability margin of a flux jumping instability is determined by the existence of a nontrivial solution of the equation [27, 28]

$$\Delta\theta - q^2\theta + \frac{nE}{\lambda} \left| \frac{\partial j_c}{\partial T} \right| \theta = 0, \quad (4)$$

where θ is the temperature perturbation, λ is the heat conductivity, E is the electric field generated by a time dependent magnetic field, the parameter q is given by

$$\tan qd = h/\lambda q, \quad (5)$$

and h is the heat transfer coefficient to the coolant. The boundary condition to Eq. (4) is $\mathbf{n}\nabla\theta = 0$ at the edge of the film and \mathbf{n} is the unit vector perpendicular to the edge of the film. It is clear from Eq. (4) that the flux front stability is highly sensitive to the electric field E generated by the varying magnetic field [26, 27, 28].

The dendrite tip motion results in an electric field \mathbf{E} , which is parallel to the current density \mathbf{j} . We consider this field similar to the consideration of the electric field generated by a varying magnetic field at a semicircular indentation with a radius ρ_0 in a superconducting film with a straight edge [28]. This approach results in

$$E \approx \dot{B}_{\text{in}} \rho_p^2 / \rho_0. \quad (6)$$

Assuming that $\rho_0 \leq \rho_p$ we estimate the magnetic field rate in the vicinity of a dendrite tip as

$$\dot{B}_{\text{in}} \approx v B_{\text{eff}} / \rho_p. \quad (7)$$

Combining the Eq. 6 and 7 we find that the electric field generated at the inner edge of a moving flux dendrite tip can be estimated as $E \approx v B_{\text{eff}} \rho_p / \rho_0$.

Next, we assume a high thermal boundary resistance in the films, which means that $hd \ll \lambda$. This assumption can be justified using typical values $\lambda = 0.1 \text{ WK}^{-1} \text{ m}^{-1}$, $d = 330 \text{ nm}$, and $h = (700 \text{ to } 1.3 \times 10^3) \text{ WK}^{-1} \text{ m}^{-2}$ [31, 32]. In this case of $hd \ll \lambda$ we find from Eq. (5) that the value of $q^2 \approx h/\lambda d$ and the stability criterion for flux jumping in thin film takes the form[28]

$$\frac{B_{\text{eff}}^2 \dot{B}_{\text{in}} n d}{2\mu_0^2 \rho_0 h j_c^2} \left| \frac{dj_c}{dT} \right| = 1. \quad (8)$$

Consider now the critical current density to be linear in temperature, *i.e.*, $j_c = j_0(1 - T/T_c)$. In this case we use Eq. (7) to rewrite Eq. (8) as follows

$$v = \gamma \frac{2\mu_0^2 j_c^2 h T_c \rho_0 \rho_p}{n d j_0 B_{\text{eff}}^3}, \quad (9)$$

where $\gamma \sim 1$ is a numerical factor and j_0 is the critical current density at $T = 0$. The criterion given by Eq. (9) gives the lower limit of a dendrite tip speed. If we assume that $\rho_0 \approx \rho_p$ and use Eq. (3) then

$$v = 2\gamma \frac{h T_c}{n d B_{\text{eff}} j_0} = 2\gamma \frac{h T_c}{n d (B_{\text{in}} - B_{\text{out}}) j_0}. \quad (10)$$

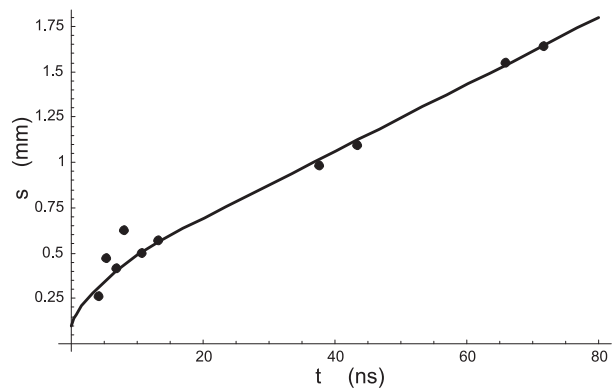


FIG. 3: The time dependence of the length of a magnetic flux dendrite $s(t)$. The solid line is the solution of Eq. (12) and the solid dots are the experimental data [15].

We compare now the results obtained by Eq. (10) and our experimental data. To measure the time dependent dendrite length $s = s(t)$ we used a magneto-optic pump-probe setup [15]. The dendrites were nucleated at the edge of a square YBCO thin film sample by focusing a laser beam onto the film surface. The magnetic field was applied prior to the laser pulse. We observed two qualitatively different stages of dendrite propagation. In the first few nanoseconds we observed an extremely high velocity on the order of 160 km/s, later on this velocity decreased to a value of 18 km/s. For experimental details see Ref. [15]. The existence of these two distinct regions of dendrites propagation can be easily understood using Eq. (10). Indeed, as long as a dendrite crosses the critical state area the field B_{out} is decreasing, therefore the value of $B_{\text{eff}} = B_{\text{in}} - B_{\text{out}}$ is increasing and consequently the velocity of the dendrite is decreasing. After the dendrite tip crosses the critical state area its velocity stays constant as the dendrite runs in a vortex free area where B_{eff} is a constant.

The time dependence of the dendrite length $s = s(t)$ can be calculated using Eq. (10). The effective field B_{eff} is the crucial parameter for this calculation. To find B_{eff} we assume that the magnetic field inside a long superconducting strip is a good approximation for the distribution at the center of a square superconducting thin film [33]

$$B_{\text{out}}(s) = \frac{\mu_0 j_0}{\pi} \begin{cases} 0, & |s| < b \\ \text{artanh}\left(\frac{\sqrt{s^2 - b^2}}{c|s|}\right), & b < |s| < a \\ \text{artanh}\left(\frac{c|s|}{\sqrt{s^2 - b^2}}\right), & |s| > a \end{cases} \quad (11)$$

where a and b are the half widths of the superconductor and of the vortex free area, and $c = \sqrt{1 - b^2/a^2}$. Substituting Eq. (11) into Eq. (10) we obtain a differential

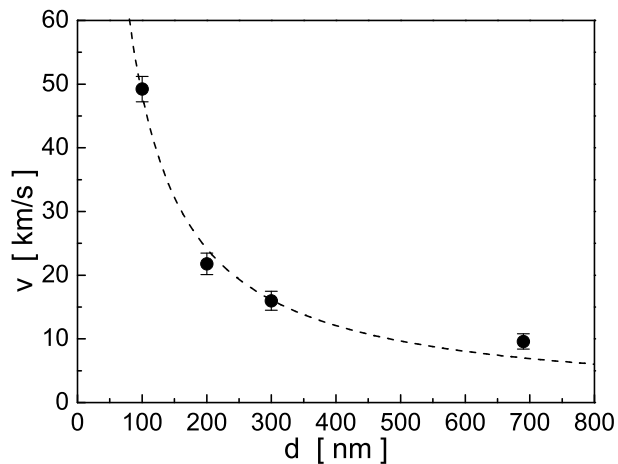


FIG. 4: The dependence of the flux dendrite velocity on the sample thickness $v(d)$. The dashed line is a fit of $v \propto 1/d$ revealing the dependence given by Eq. (7) and the solid dots are the experimental data [34].

equation for the dendrite propagation

$$\frac{ds}{dt} = \frac{\alpha}{B_{\text{in}} - B_{\text{out}}(s)}, \quad (12)$$

with $\alpha = 2\gamma h T_c / n d j_0$. Based on our experimental data we assume that the field B_{in} is constant and by a factor of 1.9 larger than the applied magnetic field.

A numerical solution of Eq. (12) yields the solid line in Fig. 3. We used for this plot the values $d = 330$ nm, $a = 5$ mm, $b = 4.4$ mm, $T_c = 90$ K, $j_0 = 1.5 \times 10^9$ A/m², $h = 10^4$ W K⁻¹ m⁻², $T_c = 90$ K, $\gamma = 1$, and $n = 6$. We take $s(0) = a - \ell$ with $\ell = 0.1$ mm as an initial condition to avoid the singularity of $B_{\text{out}}(s)$ at $t = 0$.

To check Eq. (10) further we compare the calculated velocities with the velocities obtained from line-focus measurements [15]. If a line focus is applied, the dendrites never run in the critical state, but penetrate into flux free area. In this case, as expected from Eq. (10), we don't find a regime with increased velocities, however we find a thickness dependence. In Fig. 4 one can see the experimentally obtained thickness dependent velocity and a fit $v \propto 1/d$. One reason for the slight deviations between the theory and experiment may be that we had to use different YBCO films to obtain the data, *i.e.*, the values for parameters like T_c or B_{eff} may vary.

The main result of this letter is Eq. (10). It describes the dynamics of a single flux dendrite and it was shown, that an excellent agreement with the experimental data has been achieved. To the authors' knowledge this is the

first time that a theory explains the observation of the fast and slow penetration velocities.

We want to thank the Kurt Lion Foundation, the Israeli Science Foundation (grant No 283/00-11.7), and the German Israeli Foundation (grant No G-721-150.14/10) for their support. Further, we want to thank H. Kinder for providing the YBCO samples.

* mints@post.tau.ac.il

- [1] C. P. Bean, Rev. Mod. Phys. **36**, 31 (1964).
- [2] R. G. Mints and A. L. Rakhmanov, Rev. Mod. Phys. **53**, 551 (1981).
- [3] E. Altshuler and T. H. Johanson, Rev. Mod. Phys. **76**, 471 (2004).
- [4] M. R. Wertheimer and J. le G. Gilchrist, J. Phys. Chem. Solids **28**, 2509 (1967).
- [5] M. R. Freeman, Phys. Rev. Lett. **69**, 1691 (1992).
- [6] M. R. Freeman *et al.*, IEEE Trans. Magn. **27**, 4840 (1991).
- [7] E. H. Brandt, Rep. Prog. Phys. **58**, 1465 (1995).
- [8] V. K. Vlasko-Vlasov *et al.*, Physica C **222**, 361 (1994).
- [9] M. R. Koblishka *et al.*, Europhys. Lett. **41**, 419 (1998).
- [10] R. Surdeanu *et al.*, Phys. Rev. Lett. **83**, 2054 (1999).
- [11] S. Field *et al.*, Phys. Rev. Lett. **74**, 1206 (1995).
- [12] E. R. Nowak *et al.*, Phys. Rev. B **55**, 11702 (1997).
- [13] P. Leiderer *et al.*, Phys. Rev. Lett. **71**, 2646 (1993).
- [14] C. A. Durán *et al.*, Phys. Rev. B **52**, 75 (1995).
- [15] U. Bolz *et al.*, Europhys. Letters **64**, 517 (2003).
- [16] I. Aranson, A. Gurevich, and V. Vinokur, Phys. Rev. Lett. **87**, 067003 (2001).
- [17] I. Aranson *et al.*, cond-mat/0407490
- [18] A. L. Rakhmanov *et al.*, cond-mat/0405446.
- [19] F. Bass *et al.*, Phys. Rev. B **58**, 2878 (1998).
- [20] L. M. Fisher *et al.*, Phys. Rev. Lett. **92**, 037002 (2004).
- [21] F. Bass, B. Ya. Shapiro, and M. Shvartsner, Phys. Rev. Lett. **80**, 2441 (1998).
- [22] V. Bujok *et al.*, Appl. Phys. Lett. **63**, 412 (1993).
- [23] U. Bolz *et al.*, Physica C **388**, 715 (2003).
- [24] I. A. Rudnev *et al.*, Cryogenics **43**, 663 (2003).
- [25] T. H. Johansen *et al.*, Europhys. Lett. **59**, 599 (2002).
- [26] R. G. Mints and A. L. Rakhmanov, J. Phys. D: Appl. Phys. **15**, 2297 (1982).
- [27] R. G. Mints, Phys. Rev. B **53**, 12311 (1996).
- [28] R. G. Mints and E. H. Brandt, Phys. Rev. B **54**, 12421 (1996).
- [29] J. W. Ekin, Appl. Phys. Lett **55**, 905 (1989).
- [30] R. J. Wijngarden *et al.*, Physica C **295**, 177 (1998).
- [31] J. L. Cohn *et al.*, Phys. Rev. B **45**, 13144 (1992).
- [32] M. Nahum *et al.*, Appl. Phys. Lett. **59**, 2034 (1991).
- [33] E. H. Brandt, M. V. Indenbom, and A. Forkl, Europhys. Lett. **22**, 735 (1993).
- [34] U. Bolz, Ph.D. thesis, p. 96, Konstanz (2002).